Electronic Supplementary Material (ESI) for New Journal of Chemistry.
This journal is © The Royal Society of Chemistry and the Centre National de la Recherche Scientifique 2020

Supporting Information

Optimization and gas sensing properties of Au Nanoparticles Modification α-Fe_2O_3 Nanodisk Structures for Highly Sensitive Acetone Detection

Haoyue Yang [1], Rui Zhou [1], Yongjiao Sun [1], Pengwei Li [1], Wendong Zhang [1], Zhenting Zhao [2], Jian Shi [3], Jie Hu [1,3*] and Yong Chen [3*]

[1] *Center of Nano Energy and Devices, College of Information and Computer, Taiyuan University of Technology, Taiyuan 030024, Shanxi, China*

[2] *Guangdong Provincial Key Laboratory of Electronic Functional Materials and Devices, Huizhou University, Huizhou 516001, Guangdong, China*

[3] *PASTEUR, Département de Chimie, École Normale Supérieure, PSL University, Sorbonne Université, CNRS, 75005 Paris, France*

*Author for correspondence. *E-mail:* hujie@tyut.edu.cn; yong.chen@ens.fr

S1: The intelligent gas sensing analysis system of gas sensor

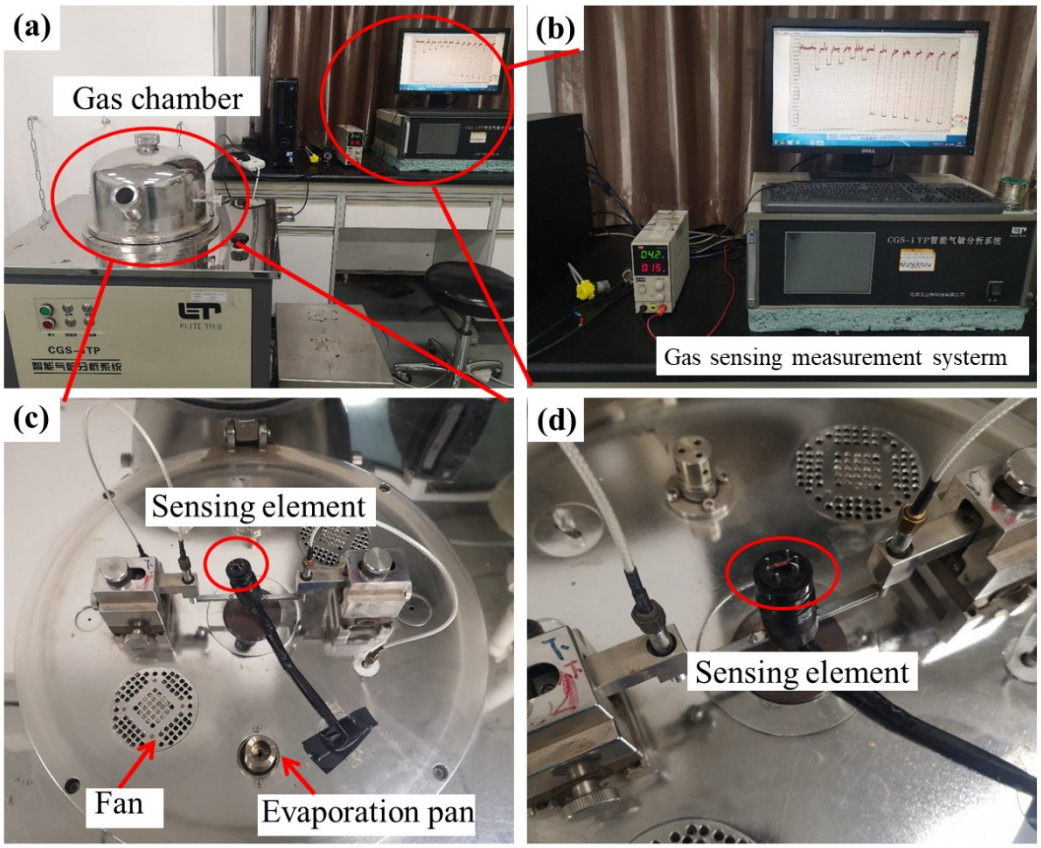

Figure S1. The intelligent gas sensing analysis system of gas sensor in our experiments.

Figure S1 illustrates the CGS-1TP intelligent gas sensing analysis system (Beijing Elite Tech Co., Ltd.), which is mainly consist of gas chamber, gas distribution system and gas sensing measurement system, as showed in Figure S1 (a). Figure S1 (b) displays the gas sensing measurement system, which used to measure the resistance change of sensor toward different concentration of acetone in real time. Figure S1 (c) exhibits the gas chamber with the volume of 18 L, which is mainly composed of the fan, evaporation pan and sensing element. Figure S1 (d) shows the magnified photo of sensing element on the pedestal of as-fabricated gas sensor.

Table S1: Acetone gas concentration comparison table

Table S1. Preparation the different concentrations of acetone in our experiment.

Acetone concentration (ppm)	Liquid acetone volume (μL)
1	32.4
5	82.08
10	32.4
50	82.08
100	32.4
200	65.7
400	65.7
600	98.55
800	87.6
1000	109.5

The process of obtaining various concentration of acetone gas is as follows: Firstly, different concentration of acetone liquid was injected into the evaporation pan in the air-filled gas chamber by a micro injector. Next the acetone liquid is transformed to gas state via heating the evaporation pan. Subsequently, the acetone gas is mixed with air by the fan. Then, the gas sensing measurement system was used to measure the sensing response of gas sensor. Table S1 shows the detail information of various gas concentrations and the liquid volume of acetone.

S2: Schematic of as-fabricated gas sensor

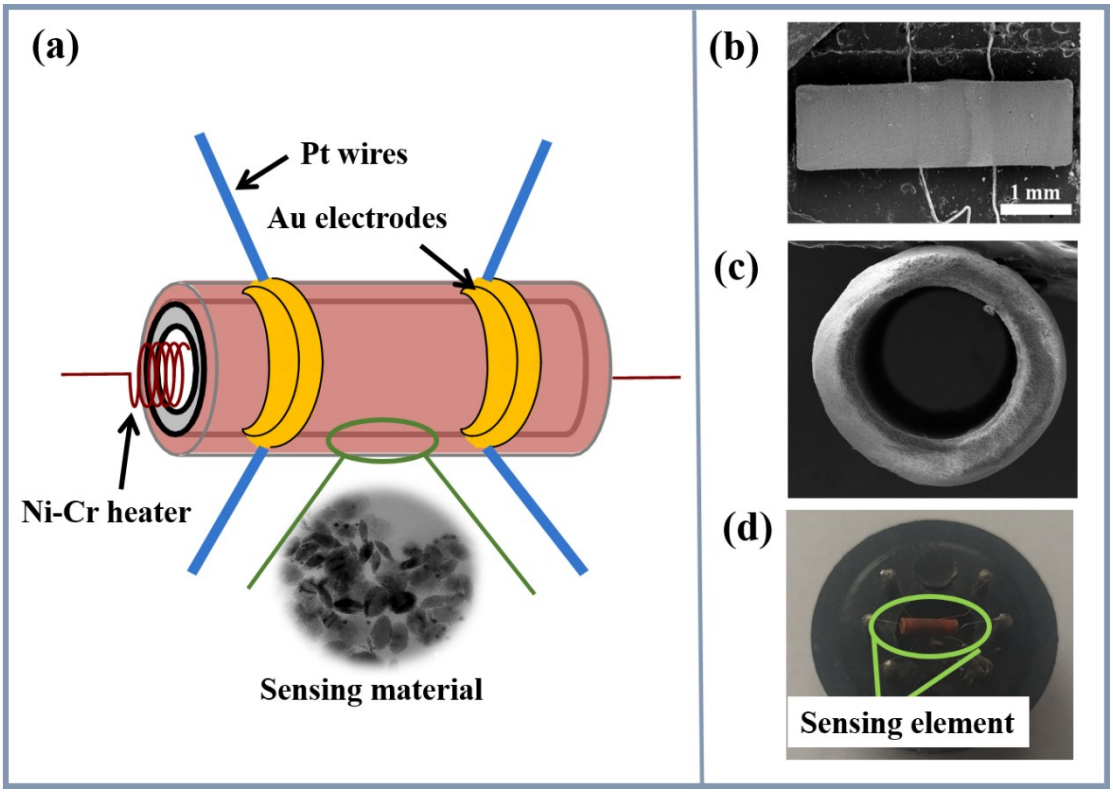

Figure S2. Schematic of α-Fe_2O_3 sensing element (a), and SEM images of α-Fe_2O_3 sensing material coating on the ceramic tube (b-c); Photograph of the integrated sensor of α-Fe_2O_3 nanodisk gas sensor (d).

We have characterized the gas sensor using schematic, SEM analysis and photograph of the integrated sensor, as shown in Figure S2 (Supporting Infprmation S2). Figure S2 (a) depicts the schematic of as-fabricated ceramic tube, which exhibited the main components including sensing material (α-Fe_2O_3 nanodisk), Ni-Cr heater, Pt wires and Au electrodes. It can be seen from Figure S2 (b-c) that the sensing material has uniformly and densely deposited on the surface of the ceramic tube, and the length of ceramic tube is about 3.8 mm. The corresponding photograph of the integrated sensor of α-Fe_2O_3 nanodisk based gas sensor is displayed in Figure S2 (d).

S3: Statistics graph of pure α-Fe_2O_3 sample

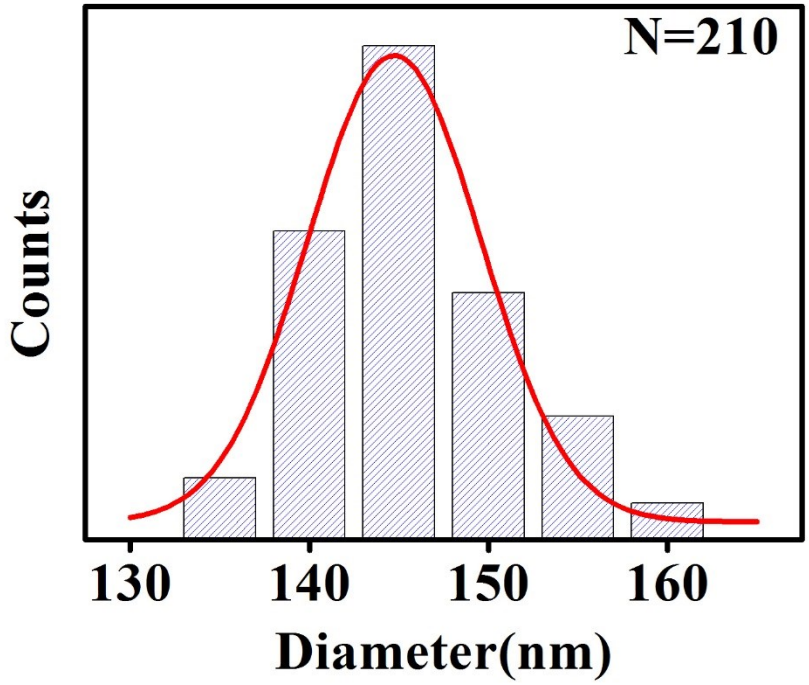

Figure S3. The statistics histogram of pure α-Fe_2O_3 nanodisk structures.

Figure S3 depicts the diameter statistics histogram of pure α-Fe_2O_3 nanodisk structures. The measured results (statistical number: 210) show that the dimension are in the range from 130 to 160 nm. Moreover, most of the dimensions of the measured samples are in the range of 140~150 nm.

S4: Dynamic resistance variation of gas sensors

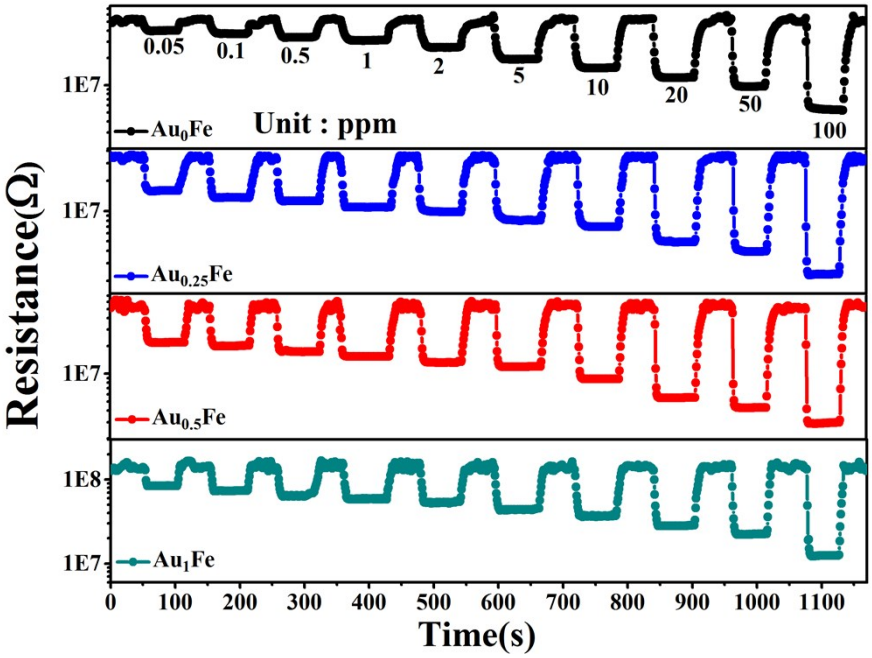

Figure S4. The dynamic resistance variation curves of as-fabricated Au_xFe gas sensors to 50 ppb~100 ppm acetone at 275°C.

The dynamic resistance variation curves of as-fabricated Au_xFe gas sensors to 50 ppb~100 ppm acetone at 275°C were shown in Figure S4. It could be observed that the resistance of the gas sensors decreased rapidly and stabled at a certain value once acetone was injected, and then they could well return to the initial resistance values (Ra) when the sensors were transferred into air. The measured results revealed that the Au_xFe gas sensors had excellent repeatability. What is more, Au NPs modified gas sensors exhibited more significant resistance variation than that of pure sensor, especially $Au_{0.5}Fe$ gas sensor kept the most distinct one toward different acetone concentration, indicating its highest acetone sensing response.

Table S2: The Ra and Rg values of as-fabricated gas sensors

Table S2. The Ra and Rg values of Au_xFe gas sensors to 50 ppb~100 ppm acetone at 275˚C.

	Rair (MΩ)				Rgas (MΩ)			
	Au_0Fe	$Au_{0.25}Fe$	$Au_{0.5}Fe$	Au_1Fe	Au_0Fe	$Au_{0.25}Fe$	$Au_{0.5}Fe$	Au_1Fe
50 ppb	53.3	35.3	58.1	151.7	39.7	15.9	21.7	84.1
100 ppb	52.9	35.6	56.2	150.6	36.8	13.6	19.7	73.1
500 ppb	52.1	35.3	58.6	149.4	33.6	12.6	17.2	63.8
1 ppm	53.2	35.4	57.2	149.5	31.1	11.1	15.4	57.7
2 ppm	52.7	35.8	58.6	154.1	25.7	9.8	13.2	53.0
5 ppm	52.4	35.2	57.6	151.7	18.8	8.2	11.9	43.1
10 ppm	52.7	35.5	56.7	146.2	15.2	6.9	8.7	37.2
20 ppm	53.1	35.1	58.1	147.2	12.2	4.9	5.4	27.9
50 ppm	54.5	35.8	58.1	146.1	9.5	3.9	4.3	22.3
100 ppm	53.4	35.8	55.8	148.3	5.4	2.3	2.9	12.5

Table S2 displayed the values of Ra (resistance in air) and Rg (resistance in acetone) of as-fabricated Au_xFe gas sensors toward 50 ppb~100 ppm acetone at 275˚C. It was noted that all the gas sensors exhibited higher resistance in air than in acetone, and Au NPs modification α-Fe_2O_3 sensors showed higher acetone sensing response (Ra/Rg) than that of unmodified sensor.

Table S3: The response/recovery times of gas sensors

Table S3. The response/recovery times of as-fabricated sensors toward 50 ppm acetone at 275˚C.

	Au_0Fe	$Au_{0.25}Fe$	$Au_{0.5}Fe$	Au_1Fe
τ_{res}	5	4	4	4
τ_{rec}	11	9	7	7

Table S3 illustrates the detailed response/recovery times (τ_{res}/τ_{rec}) of as-fabricated sensors toward 50 ppm acetone at 275˚C. Clearly, response/recovery times of Au_0Fe, $Au_{0.25}Fe$, $Au_{0.5}Fe$ and Au_1Fe sensors were 5 s /11 s, 4 s /9 s, 4 s /7 s and 4 s /7 s, respectively. Notably, the Au NPs modification α-Fe_2O_3 sensors exhibited shorter response/recovery times than that of pure one, and the measured results indicated that the introduced of Au could greatly improve the properties of response/recovery times.